J Mater Sci (2012) 47:960–968
DOI 10.1007/s10853-011-5875-z

Effect of pre-strain on grain size distributions in 316H austenitic stainless steel

S. Mahalingam · P. E. J. Flewitt · J. F. Knott

Received: 18 July 2011 / Accepted: 11 August 2011 / Published online: 31 August 2011

Abstract An experimental study addressing the effect of tensile deformation on recrystallized grain size has been undertaken to explore the conditions leading to abnormal grain growth in Type 316H austenitic stainless steel. Following a solution heat treatment, a Type 316H stainless steel has been subjected to various tensile deformations up to a maximum of approximately 50% strain and then heated at a temperature of 1150 °C for 0.5 h followed by furnace cooling. A fraction of abnormally large grains is observed following a prior strain of approximately 20%. The results are presented, in terms of standard statistical analysis, and also graphically. The graphical presentation provides a clear, visual appreciation of uni- and bi-modal distributions, which may be of general help in other analyses of this nature.

Introduction

Most engineering metals and alloys are polycrystalline and the grains are separated from one to another by defined boundaries. It is these grain boundaries that influence the mechanical, physical and chemical properties of the material [1]. Grain growth at elevated temperatures has been studied extensively since it results in a reduction in the total energy of the material through a decrease in grain boundary area per unit volume [2]. In general for polyhedral 3D grains there is a relationship between the number of grain faces, edges and vertices [3]. Various mechanisms have been proposed for grain growth including migration of the curved boundaries towards the centre of curvature whilst maintaining the balance of tensions at the grain edges. It is well established that deformation before heat treatment can lead to abnormally large grains forming at a critical value of strain. However, if this critical value is exceeded a relatively uniform distribution of grains is formed [4].

The classical model for describing the effect of grain size on the yield strength of materials was established by Hall [5] and Petch [6]. More recently, Druce [7] showed that prior austenite grain size determines the brittle and ductile properties of MnMoNi steels. The effect of grain size distribution on yielding has been investigated by Kurzydlowski [8] who identified the importance of both mean grain size and the width of the grain size distribution. Ramtani et al. [9] concluded that a bi-modal grain size distribution demonstrated better ductility than a uni-modal grain size in ultra-fine-grained nickel.

The grain size distribution is one of the typical and fundamental properties for analyses aimed at the characterisation of the microstructure of materials. The two dimensional (2D) grain size distributions cannot be related directly to the changes taking place in three dimensions (3D). Therefore, statistical and geometrical criteria are used to calculate the 3D spatial distribution from experimental 2D data [10]. Several methods have been proposed to determine the 3D spatial grain size distribution from 2D size distributions of the sections where grain diameter is

S. Mahalingam (✉) · P. E. J. Flewitt
Interface Analysis Centre, University of Bristol,
Bristol BS2 8BS, UK
e-mail: Sunthar.Mahalingam@bristol.ac.uk

P. E. J. Flewitt
School of Physics, H H Wills Physics Laboratory,
University of Bristol, Bristol BS8 1TL, UK

J. F. Knott
School of Metallurgy and Materials, College of Engineering
and Physical Science, University of Birmingham, Birmingham
B15 2TT, UK

Table 1 Chemical composition of 316H austenitic stainless steels (wt%)

C	Si	Mn	P	S	Cr	Mo	Ni	Al	B
0.05	0.58	1.65	0.016	0.005	17.4	2.42	11.6	<0.010	0.005
Co	Cu	Nb	Sn	Ti	V	W	N	Ta	Fe
0.04	0.07	0.01	<0.01	0.01	0.02	0.01	0.041	<0.01	Bal

measured on the cross-section of the samples [11]. Of these the Schwartz–Saltykov method provides a realistic estimation of the 3D size distribution but it is necessary to have the statistical distributions to describe microstructure with homogeneous and inhomogeneous grain sizes and classes [12]. An accurate mathematical description of the grain size statistics is necessary to correlate the effect of grain size with properties of materials. The measured grain sizes in polycrystalline materials are generally considered to conform to a statistical log-normal distribution [13].

Smith analysed the topology of grains and based on experimental results concluded that the polyhedral grain shape is determined by the requirements of both space-filling and minimising surface energy [3]. For size distribution characterisation one approach was to invoke a simple approximation of the polyhedral grains to spherical grains. Exner [14] evaluated the experimental methods for data collection and mathematical solutions to determine spatial grain size distributions. Tweed et al. [15] assessed the grain size distribution during the grain growth of aluminium-alumina alloys and distinguished between different types of grain growth mechanisms. This study considered the influence of various microstructural parameters on the normal to anomalous grain growth transition. In general abnormal grain growth has been observed in a range of polycrystalline metals and alloys including, for example, relatively pure metals such as copper, and also alloys based on Ti and Al [16]. As pointed out by Ralph [17] the causes that lead from normal to abnormal grain growth are complex. Some experimental investigations are described by Humphreys [18] and a theoretical analysis is given by Srolovitz et al. [19].

Type 316H austenitic stainless steel is used widely for a range of high temperature engineering components [20]. Hence, it is important to understand the contribution of deformation before heat treatment that may lead to phenomenon of abnormal grain growth in this material. The aim of this article is to study the effect of pre-strain on grain growth in a 316H austenitic stainless steel, and to use appropriate statistical techniques to test the assumption of a ''log-normal'' distribution for grain size. An interesting finding, related to one particular percentage of pre-strain, enables the techniques to be extended to establish the existence of a bi-modal grain-size distribution.

Experimental procedure

Material

A type 316H austenitic stainless steel extracted from an ex-service Advanced Gas Cooled Reactor super-heater header was supplied by EDF Energy (UK). The chemical analysis for this material is given in Table 1. The initial block of material ($120 \times 100 \times 70$ mm^3) was solution heat treated at a temperature of 1090 °C for 2.5 h and then water quenched to room temperature. This heat treatment produced a single phase austenitic microstructure with a 2D grain size of approximately 112 μm.

Pre-straining and grain size measurement

Tensile test specimens with 4 mm diameter and 30 mm gauge length were machined from the austenitic stainless steel block. The specimens were plastically deformed at room temperature in tension using an Instron servo-hydraulic machine at a strain rate of 0.001 s^{-1} under displacement control. Subsequently, the cold worked specimens with various plastic strain levels 0%, 10.4%, 16.4%, 20.3%, 33.3%, and 49.2% were heat treated at a temperature of 1150 °C for 0.5 h and then furnace cooled. They were sectioned and metallurgically prepared to a 1 μm finish and then electrolytically etched using a 2% oxalic acid solution at 10 V dc. An Olympus BH-2 optical microscope was used to examine the microstructures. Two-dimensional grain size measurements were made on the optical micrographs using the linear intercept method within the ImageJ program [21]. The procedure adopted ensured that the measurements of grain size accommodated annealing twins and therefore a true representation of grain size was achieved. Scanning electron micrographs of some samples were also taken in the back scattered mode using a Hitachi S-2300 SEM. This instrument was fitted with an energy dispersive microanalyses spectrometer (Link Systems).

The grain size distribution from 2D images was obtained by dividing the grain size into a number of class intervals. The spatial size distributions of the overall grain structure were determined from 250 measurements on each sample, thereby establishing the statistical variation of grain size

caused by metallographic sectioning. Log-normal probability plots have been used to fit the data justifying the log-normal behaviour of grain size distribution since these plots provide an easy-to-visualise representation of the data. The Schwartz–Saltykov method was used to obtain the spatial size distribution assuming that the polyhedral grain structure may be approximated to a poly dispersed system of sectioned spheres [12]. All the grain size data were fitted to a log-normal distribution using the Matlab software.

Two forms of statistical analysis are used. One is the probability distribution function (pdf) where the distribution of the grain size is given by an assumed log-normal distribution function,

$$p(D:S,M)=\frac{1}{S\sqrt{2\pi D}}\exp\left[-\frac{1}{2}\left(\frac{\log_{10}(D)-M}{S}\right)^2\right] \quad (1)$$

The other is the cumulative distribution function (CDF) which has the form,

$$\mathrm{CDF}(D:S,M)=\frac{1}{2}\left(1+\mathrm{erf}\left(\frac{\log_{10}(D)-M)}{S\sqrt{2}}\right)\right) \quad (2)$$

where D is the experimentally measured diameter of each grain, and M and S are parameters characterising the log mean grain size and log standard deviation of the log-normal distribution, respectively.

Results

Prior deformation and heat treatment

Figure 1 shows the typical stress–strain curve taken to 49.2% strain for the 316H austenitic stainless steel. The corresponding interrupted strain levels used for subsequent heat treatment are also indicated. The yield strength of ~250 MPa corresponds with the values obtained for similar material in the literature, however, the UTS value of ~600 MPa is towards the lower bound [22]. Figure 2 shows typical microstructures at different stages after strain-annealing at a temperature of 1150 °C for 0.5 h. The unstrained water quenched specimen, Fig. 2a shows austenite grains containing annealing twins and some inclusions. These inclusions were found to be either sulphide or oxide by energy dispersive X-ray microanalysis. Successive increases of strain followed by annealing produce a similar uniform grain distribution up to 16.4%. At the critical strain level of 20.3% substantial grain growth occurs. Some of the grains have become abnormally large relative to the surrounding smaller grains, Fig. 2b. The larger grain in the, 2D section, Fig. 2b has a nominal maximum dimension of about 300 μm and irregular

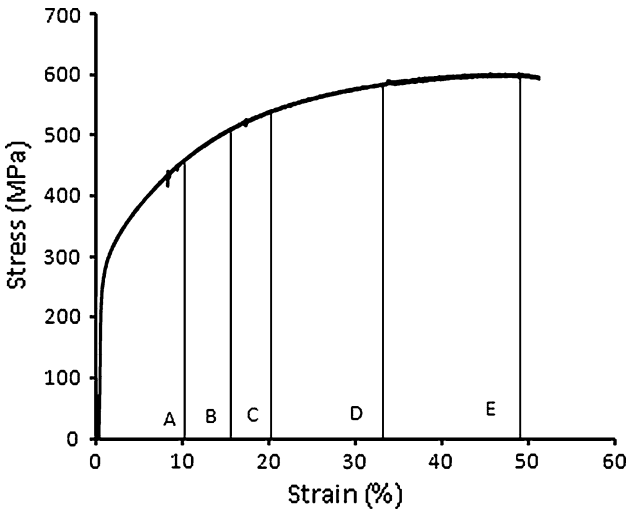

Fig. 1 Stress versus strain plot for the Type 316H austenitic stainless steel; *vertical line* shows the strains before subsequent heat treatment: *a* 10.4%, *b* 16.4%, *c* 20.3%, *d* 33.3%, and *e* 49.2%

boundaries to accommodate the match with the surrounding grains. Figure 2c shows the microstructure typical of the higher strain levels ≥33.3% where a uniform grain microstructure is present.

Grain size

Figure 3b shows the histograms of 2D grain size measurements for each level of strain-annealing. These distributions are uniform and similar at pre-strain levels up to 16.3%, Fig. 3a–c. At the strain level of 20.3% the distribution is markedly different, Fig. 3d. The grain size distribution here suggests anomalous grain growth. The individual size distributions obtained at the higher strain levels Fig. 3e, f have characteristics comparable to lower strain levels.

Figure 4 shows the log-normal probability plots for the 316H austenitic stainless steels where the logarithmic grain sizes are plotted against the cumulative frequency. The median rank of order number n in a total population of N, Fn, is given by [23]:

$$\mathrm{Fn}=\frac{(n-0.3)}{(N+0.4)} \quad (3)$$

It is noted from Fig. 4a–f that within the experimental error most data points follow a straight line apart from Fig. 4d. In the other cases for each grain size distribution there is only a small deviation at the smaller- and larger-grain sizes.

The mean 2D grain sizes were obtained from the 0.5 probability of the cumulative frequency and the standard deviation is located at 0.16 and 0.84 on (the log normal) CDF plots. The "spread'' of the distributions derived from

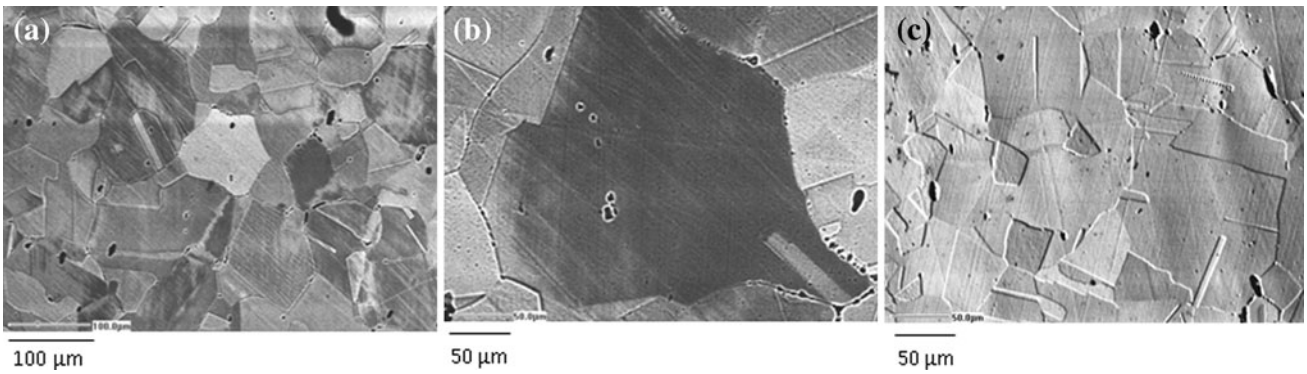

Fig. 2 Scanning electron back-scattered micrographs of plastically deformed and annealed specimens **a** 0% **b** 20.30% **c** 33.30%. Note differences in magnification between **a**–**c**

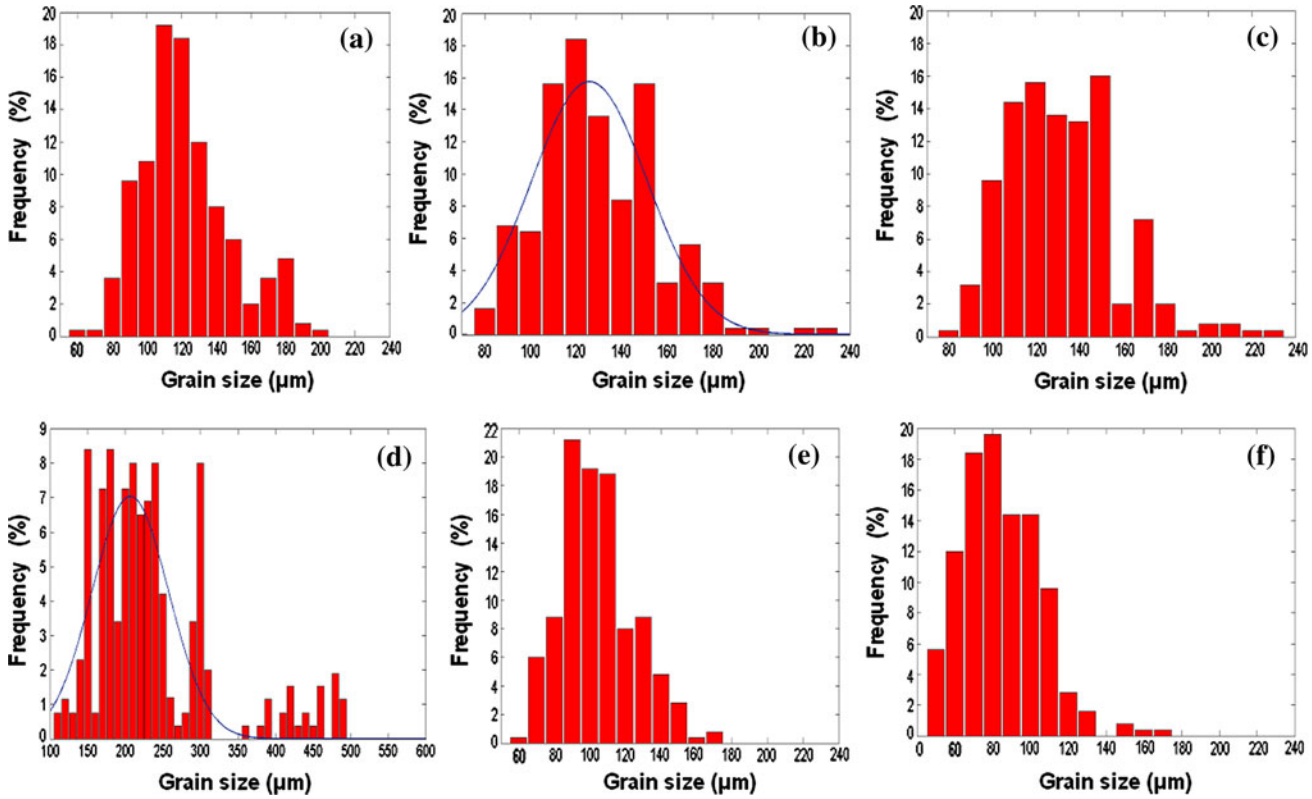

Fig. 3 Histogram showing the measured grain sizes for strains of **a** 0% **b** 10.4% **c** 16.4% **d** 20.3% **e** 33.3% **f** 49.2%. Note change of scale on the abscissa for Fig. 3d

these standard deviations are converted into "linear space'' from the "log normal space''. For example for 0%, log mean is 2.086. The symmetrical log standard deviation values corresponding to 0.16, 0.84 are 1.99, 2.173, respectively. These give grain sizes of 98, 149 µm with a spread of 51 µm in linear space. The "spread'' values for the different pre-strains are shown in Table 2.

The maximum grain sizes were obtained at a pragmatic value of 99.9%, arguing that when the chance of occurrence of "super-maximum'' size grain is less than 0.1% there would be so few in the microstructure that any affect on bulk, averaged properties, such as flow stress, should be minimal.

Figure 4d shows that when the experimental data are treated as a uni-modal distribution there is a departure from linearity when the grain size is large; clearly the data points do not follow a straight line. There is a pronounced change in slope at the two branches of the uni-modal distribution between grain sizes 100–350 and 350–600 µm. This observation is similar to the finding from the Wu and Knott [24] statistical analysis of local fracture stresses in notched bars

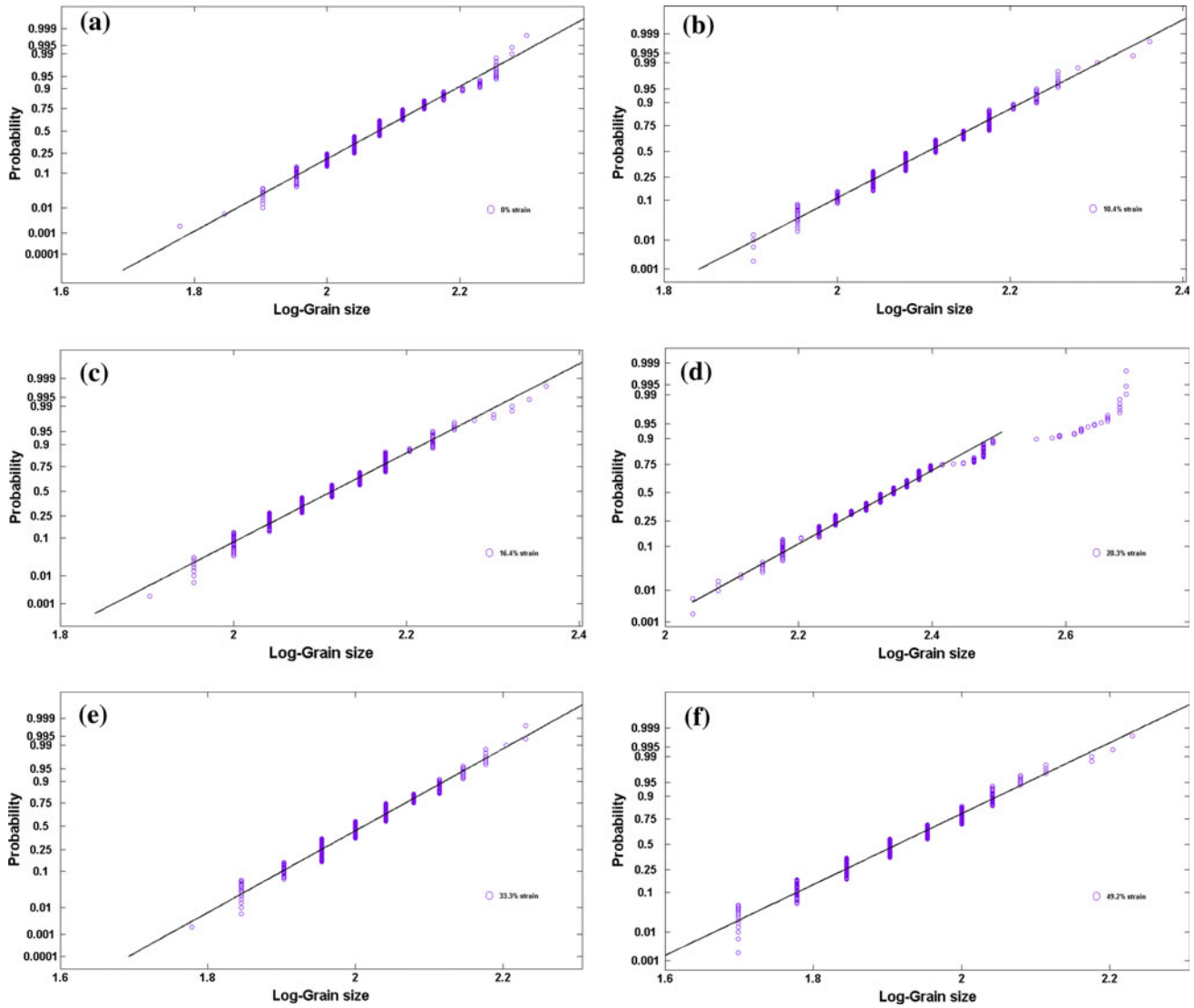

Fig. 4 Log-normal cumulative probability plots for two dimensional grain size distributions for strains of **a** 0% **b** 10.4% **c** 16.4% **d** 20.3% **e** 33.3% **f** 49.2%

Table 2 The characteristics of log-normal probability plots for two dimensional grain size distributions

Degree of deformation (%)	Mean grain size (μm)	Width or spread of the distribution (μm)	Maximum grain size (μm)
0	122	51	230
10.4	130	53	245
16.4	132	49	245
20.3	215	112	580
33.3	104	41	195
49.2	85	42	180

where they deliberately combined two distinct local fracture stress distributions as a single population. This prompted a re-analysis of the data in Fig. 4d, as described below.

Figures 3b, d show the 2D log-normal grain size distributions superimposed on the histograms of 2D measurements. The 2D and the 3D log-normal grain size distribution fits to the experimental data in Fig. 3 are given in Fig. 5. The 3D size distributions were derived from the 2D distributions using the procedure described by Underwood [11] and DeHoff and Rhines [12]. The statistical 2D and 3D mean grain sizes and standard deviations (derived from "log-normal space'') for the different pre-strains are given in Table 3. This Table also shows the goodness of fit to the data and the χ^2 tests for the fitted log-normal distributions. There is very good fit to the experimental data in all cases apart from one case: the 20.3% pre-strain. In all other cases, R^2 is greater than 0.86. This was validated by drawing the random samples from each population and finding their χ^2 values. The probability that

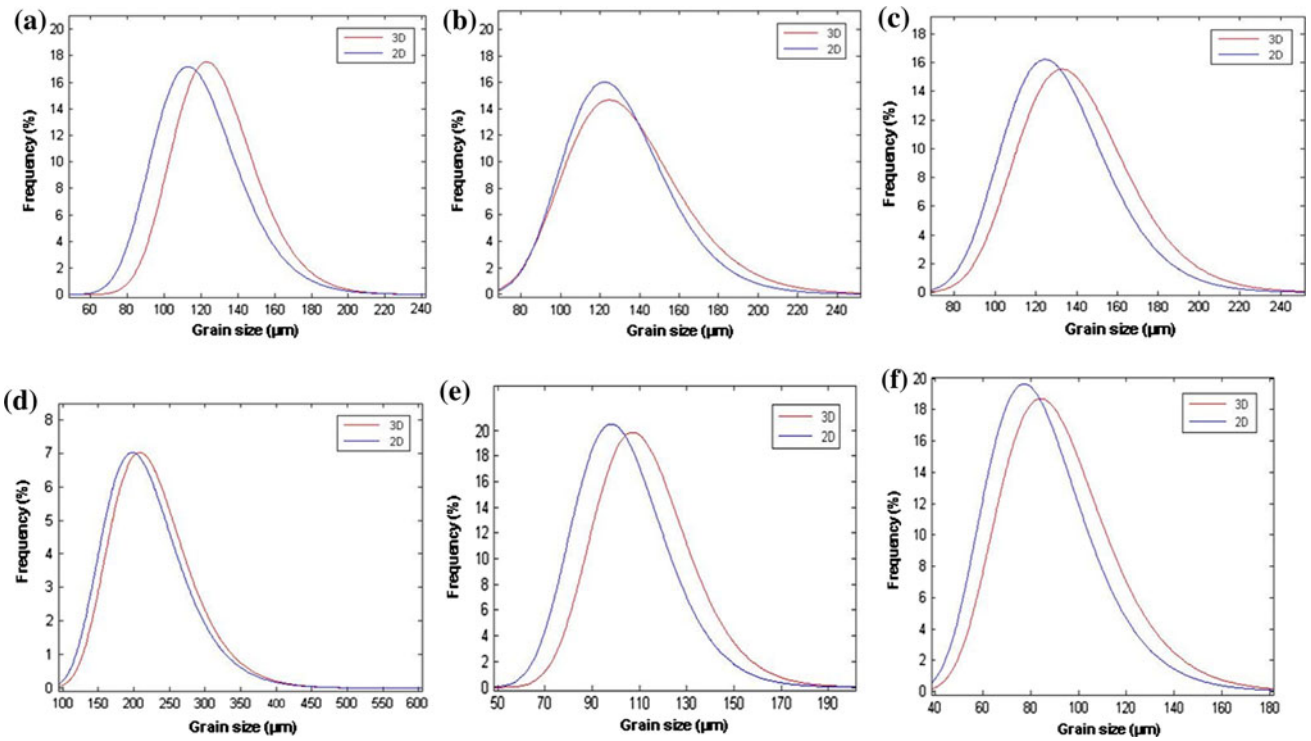

Fig. 5 Log-normal two dimensional and three dimensional grain size distributions for strains of **a** 0% **b** 10.4% **c** 16.4% **d** 20.3% **e** 33.3% **f** 49.2%. Goodness of fit to the data in Fig. 3 for each distribution is given in Table 3

sampling is rejected is less than 0.005. For the lower deformations, including 0%, a characteristic uni-modal distribution provides a good fit to the experimental data that can be attributed to a homogeneous microstructure arising from normal grain growth, Fig. 4a–c. At higher degrees of deformation, Fig. 4e, f, again a uni-modal distribution provided a good fit to the data. However, in the case of the experimental data for the pre-strain level of 20.3% treated as a uni-modal distribution, Fig. 4d, the goodness of fit of 0.64 is poor. This poor fit is very evident from the comparison in Fig. 3d, where larger grain sizes are not accommodated. The probability of χ^2 tests also showed that the random sampling rejected will be high. This prompted the treatment of these experimental data as a special case since Fig. 3d is portraying potential bi-modality.

The observed departure from linearity in Fig. 4d led to a reconsideration of the experimental data as two distributions. The reconstruction of CDF plots are shown in Fig. 6a, where two linear plots are present which overlap (Region X). The fit to the data was optimised by considering several divisions of this data set. This provides a visualisation for the distributions and it is very clear that a sharp change in the slope is observed and all data fit with one distribution or the other even in Region X; the two overlapping distribution tails. The experimental data for the pre-strain level of 20.3% were reanalysed treating as a bi-modal distribution. Figure 6b shows the bi-modal distribution which is indicated by two peaks: a prominent peak at $\sim$215 μm mean grain size and a smaller peak at $\sim$460 μm mean grain size. This analysis validated the

Table 3 The characteristics of log-normal two and three dimensional grain size distributions

Degree of deformation (%)	Mean grain size (μm)		Width or spread (μm)		Goodness of fit (R^2)	χ^2 value
	2D	3D	2D	3D		
0	115	125	51	49	0.94	53.34
10.4	124	128	53	55	0.86	53.08
16.4	127	135	49	52	0.89	53.54
20.3	204	214	112	113	0.64	8.19
33.3	100	109	41	40	0.95	37.97
49.2	80	87	42	40	0.97	40.45

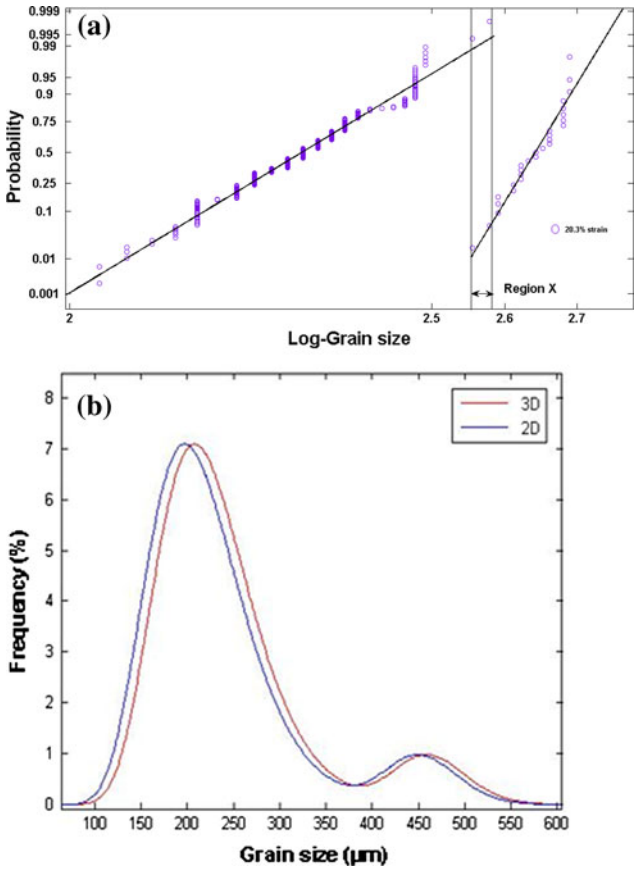

Fig. 6 Bimodal representation of strain level of 20.3% **a** Log-normal cumulative probability plot **b** Log-normal grain size distribution

inhomogeneity in the microstructure which arose from the abnormal grain growth.

Discussion

The theory derived by Schwartz–Saltykov used to fit the log-normal distribution to the measured grain sizes is based upon sectioning of spherical grains. This is recognised to be a reasonable approximation when considering regular polyhedral grains in a polycrystalline material. The values of R^2 and χ^2 in Table 3 and the linearity of the CDF plots in Fig. 4 support the log-normal distribution for the 3D unimodal grain distributions observed in the present experiments. For the first three entries in Table 3, it is clear that there is insignificant change in mean grain size or standard deviation: the plots in Fig. 4a–c are linear and parallel. Moreover, when a bi-modal distribution is de-convoluted into its constituent parts, as described above, it is clear that both the individual distributions are log-normal, Fig. 6a. The sectioning of spherical grains is an approximation that enables both a mean and a maximum grain size to be evaluated [12]. The means are obtained from 0.5 probabilities in the cumulative distributions in Fig. 4 and the peaks in the log-normal distributions shown in Fig. 5. These have been derived by converting the "log-normal space'' values into "linear space''. The maximum grain size is obtained from the upper tail of the log normal distribution and the corresponding probability of 99.9% for the cumulative distribution. The values for the mean distributions and the corresponding "spreads'' are given in Tables 2 and 3. It is not easy to establish the upper limit from the log-normal distribution plots but this can be readily obtained from the cumulative distributions, Fig. 4. The individual (straight) lines can be simply extrapolated to a pragmatic probability value of 99.9% and the corresponding values can be measured directly. Such values are shown in Table 2. In the case of the bi-modal distribution of grain sizes, Fig. 5d, these values are readily obtained even where there is overlap of the tails of the distributions as shown in region X of Fig. 6a.

The analyses adopted to interrogate the 316H austenitic stainless steel data point to the importance of the appropriate statistical representation to evaluate the mean grain size and maximum grain size in polycrystalline materials. Although the two procedures described are based upon a log-normal distribution of grain size, the CDF presentation assists in visualising the output of the statistical analyses: in particular, it greatly simplifies the estimation of maximum grain size, through linear extrapolation to 99.9%; the linear fit to data supports the log-normal distribution.

The results of the grain size measurements following straining and annealing demonstrate that at a critical strain of $\sim$20% there is a bimodal distribution of grain sizes, Fig. 6a, b. Grain size measurements up to, but not including this value, of critical strain produce well defined single distributions Figs. 5a–c. As shown in Table 3 the 3D distributions of grain size give mean values of 125, 128, and 135 μm with "spreads'' of 52, 56, and 52 μm, respectively. For strains exceeding the critical value the overall mean grain size decreases from 109 to 87 μm for strains of 33.3 and 49.2%, respectively. Again when taking into account the associated values of "spreads'', Table 2, there is no significant difference in the grain sizes. These reduced grain sizes are consistent with recrystallization arising from an increased number of nucleation sites present as a result of the associated greater density of dislocations at these higher levels of strain [25].

The grain growth process is generally divided into two parts: normal and abnormal. For normal grain growth the grain size distributions remain the same shape and moves to larger sizes as a function of time and temperature [26]. The outcome of the three dimensional statistical analyses at the critical strain of 20.3% is instructive since it reveals significant growth associated with the smaller of the two grain populations with a mean of 214 μm and a maximum

of 380 μm and the abnormally larger population with a mean of 462 μm and a maximum of 580 μm. Inspection of the standard deviations shows these differences to be statistically significant. In each case the two populations have a mean and maximum grain size that is greater than that measured in the strain range 0–16.4%. The "abnormally large'' population is approximately 7% of the total volume of material based upon the relative areas under the two 3D distribution peaks shown in Fig. 6b. The corresponding log-normal cumulative probability plot, Fig. 6a, provides an excellent visual confirmation of the bi-modal distribution. Indeed in the range of overlap of the tails of the two distributions, region X, this plot shows that linearity is retained supporting the bi-modal interpretation.

In general previous considerations of anomalous grain coarsening have shown a systematic increase in grain size from ~100 μm to a point below the peak associated with the critical strain [27]. Post peak the grain size has decreased monotonically. At the critical strain the subsequent heat treatment has produced a uni-modal but anomalously large size distribution of grains. By comparison the present results show that this trend is not followed, but rather at the 20.3% strain there is a bi-modal distribution of sizes, Fig. 6b. The majority of grains have coarsened to a mean of ~214 μm a maximum of ~380 μm. However, there is an additional, but small, proportion of larger grains of mean size of ~462 μm and a maximum of 580 μm.

The abnormal grain growth observed in this case is where the uni-modal grain size distribution turns into the bi-modal distribution. This study has concentrated on the measurement of grain size and not the underlying mechanisms. However, the observed variations of grain size are broadly consistent with previously identified mechanisms of grain coarsening and indicate the growth of new grains during recrystallization. Within the 316H austenitic stainless steel following the solution heat treatment there are only a few widely distributed inclusions present, Fig. 2, hence any grain boundary pinning provided by these inclusions would be limited and therefore insignificant in inhibiting overall boundary migration [28]. In addition, although the sulphide and oxide inclusions have different coefficients of thermal expansion there is no evidence that any mismatch strain contributes to the formation of the abnormally large grains [29]. Hence both the overall grain growth and the production of abnormally large grains are most probably related to stress driven grain boundary migration [30]. Here, the increase of plastic deformation causes more strain accommodation at the boundaries and the strain variation plays a prominent role in grain growth. The dislocations created or annihilated within the grain boundaries increase boundary migration mobility by facilitating release of the boundary from pinning sites. This will be dependent upon the orientation of the individual grain boundaries. Since there is a distribution of orientations in such a polycrystalline material will leave some boundaries with a significantly lower resistance to migration. It is this that has the potential to promote growth for certain grains to an abnormally larger size.

Conclusions

We may draw the following conclusions from this study.

- Pre-strains up to ~50% influenced the size of the grains produced in a 316H austenitic stainless steel subsequently heat treated at 1150 °C for 0.5 h.
- The 3D grain sizes derived from the 2D measurements followed a uni-modal log-normal type distribution for both low and high pre-strains.
- Normal grain growth occurred at all strain levels except at 20.3% strain where abnormal grain growth was observed.
- For a strain of 20.3% the grain size distribution is characterised by a bimodal log-normal distribution with grain growth combined with the formation of abnormally large grains of diameters 462 (mean) and 580 μm (maximum). The latter representing about 7% of the total population.
- The application of two related statistical procedures provide a helpful method for analysing the bi-modal grain size distribution. In particular, the CDF, plotted graphically, allows the uni- and bi-modal log-normal distributions to be viewed simply as straight lines, showing the mean at 0.5, the standard deviation at 0.16 and 0.84, and enabling simply extrapolation to a specified limit (set at 99.9%) to obtain a "pragmatic" maximum grain size.

Acknowledgement The authors acknowledge the EPSRC for financial support (Grant EP/H006729/1) and EDF Energy Ltd for the provision of the material.

References

1. Flewitt PEJ, Wild RK (2001) In: Grain boundaries: their microstructure and chemistry. John Wiley & Sons Ltd., Chichester
2. Smith CS (1948) In: Metals technology, vol 175. Trans AIME, New York, pp 15–51
3. Smith CS (1952) In: Metal interfaces, ASM, Cleveland, pp 65–113
4. Randle V (1993) Mater Sci Forum 113–115:189
5. Hall EO (1951) Proc Phys Soc Ser B 64:747
6. Petch NJ (1953) J Iron Steel Inst 174:25
7. Druce SG (1986) Acta Metall 34(2):219
8. Kurzydlowski KJ (1990) Scr Metall Mater 24(5):879
9. Ramtani S, Dirras G, Bui HQ (2010) Mech Mater 42(5):522

10. Moore PG (1969) In: Principals of statistical techniques. Cambridge University Press, Cambridge
11. Underwood EE (1970) In: Quantitative stereology. Addison-Wesley Publishing Company, Reading
12. DeHoff RT, Rhines FN (1968) In: Quantitative microscopy. McGraw-Hill, New York
13. Berbenni S, Favier V, Bui HQ (2007) Int J Plast 23(1):114
14. Exner HE (1972) Int Metall Rev 17(1):25
15. Tweed CJ, Hansen N, Ralph B (1985) Metallography 18(2):115
16. Koo JB, Yoon DY, Henry MF (2002) Metall Mater Trans A 33A:3803
17. Ralph B (1990) Mater Sci Technol 6:1139
18. Humphreys FJ (1992) Mater Sci Technol 8:135
19. Srolovitz DJ, Grest GS, Anderson MP (1985) Acta Metall 33(12):2233
20. Marshall P (1984) In: Austenitic stainless steels: microstructure and mechanical properties, Elsevier Applied Science Publishers, Barking
21. Muirhead J, Cawley J, Strang A, English CA, Titchmarsh J (2000) Mater Sci Technol 16(10):1160
22. Turski M, Bouchard PJ, Steuwer A, Withers PJ (2008) Acta Mater 56(14):3598
23. Bompas-Smith JH (1983) In: Mechanical survival: the use of reliability data. McGraw-Hill, New York
24. Wu SJ, Knott JF (2004) J Mech Phys Solids 52(4):907
25. Abbaschian R, Abbaschian L, Reed Hill RE (2009) In: Principles of physical metallurgy. Cengage Learning, New Delhi
26. Hillert M (1965) Acta Metall 13(3):227
27. Chang CH (2000) Fatigue crack growth in simulated HAZ structures of stainless steel weldments. PhD Thesis, The University of Birmingham
28. Randle V, Ralph B (1986) Acta Metall 34(5):891
29. Tweed JH, Knott JF (1986) Acta Metall 35(7):1401
30. Sharon JA, Su PC, Prinz FB, Hemker KJ (2011) Scr Mater 64(7):25